INTERNATIONAL JOURNAL OF INTEGRATED ENGINEERING
ISSN: 2229-838X e-ISSN: 2600-7916

IJIE

Vol. 16 No. 9 (2024) 67-79
https://publisher.uthm.edu.my/ojs/index.php/ijie

Calcined Waste Marsh Clam Shell in Various Combustion Temperatures as Phosphate Removal in Water

Nur Husna Muslim[1]*, Abdul Aziz Maryani[2], Nur Aqilah Hisham[2], Muhammad Ariff Aiman Mohd Radzi[2], Noorul Hudai Abdullah[2]*, Nur Atikah Abdul Salim[3], Norzainariah Abu Hassan[4]

[1] *Faculty of Engineering Technology, Universiti Tun Hussein Onn Malaysia, Hab Pendidikan Tinggi Pagoh, Km 1, Jalan Panchor, 84600 Muar, Johor, MALAYSIA*
[2] *Neo Environmental Technology, Centre for Diploma Studies, Universiti Tun Hussein Onn Malaysia, Pagoh Education Hub, 84600 Pagoh, Johor, MALAYSIA*
[3] *School of Occupational, Safety & Health, Netherlands Maritime University College, Johor Bahru, Johor, 80000 MALAYSIA*
[4] *Department of Civil Engineering, Politeknik Melaka, No. 2, Jalan PPM10, Plaza Pandan Malim 75250 Melaka, MALAYSIA*

*Corresponding Author: nurhusnabintimuslim@gmail.com; noorul@uthm.edu.my
DOI: https://doi.org/10.30880/ijie.2024.16.09.005

Article Info

Received: 26 January 2024
Accepted: 11 September 2024
Available online: 4 December 2024

Keywords

Calcined marsh clam shell, phosphate, isotherm, kinetic, solution

Abstract

Phosphate ranks among the major pollutants in water that might cause eutrophication in the receiving bodies of water. Excessive phosphate can stimulate algae blooms and deteriorate the water ecosystem's quality. Many techniques focus on phosphate removal by using biological, physical, or chemical treatments. However, the application of the adsorption mechanism using calcined marsh clam shells (CMCs) remains insufficiently researched in terms of various calcination temperatures. Hence, the ability of CMCs calcined at different temperatures was investigated to determine their potential to remove phosphate from aqueous solutions. The adsorbent materials were calcined at four variety of temperatures: 500, 600, 700, and 800°C. In the batch experiment, 2 g of mass of absorbent in the size range of 1.18–2.36 mm was mixed with 100 mL of solution. The physical and chemical characteristics of adsorbents were characterised to determine the surface morphology, functional groups, and elemental composition. The calcination temperature of 600°C resulted in the most effective adsorbent for phosphate removal (99.53%). Kinetic (pseudo-first-order and pseudo-second-order) and isotherm (Freundlich and Langmuir) models were implemented to identify the adsorption mechanisms. The data fitted well to the pseudo-second-order kinetic model, indicating that the process is a chemical sorption process. The Freundlich isotherm model described the phosphate adsorption onto CMCs well, which indicates multilayer adsorption of phosphate on the CMCs surface layer. Overall, applying the different types of CMCs can enhance phosphate removal due to the capability of adsorption on surface materials and an advanced understanding of the validated data using kinetic and isotherm models.

1. Introduction

Phosphate is a non-metallic chemical with the symbol P below nitrogen in group 15 of the periodic table that appears in both particulate and dissolved forms in natural waterways [1]. Phosphate is an essential nutrient for plants (algae) and other organisms. Phosphates are usually found in the environment in the form of orthophosphates, organic phosphates, or polyphosphates [2]. However, increased phosphate content in wastewater rapidly stimulates the growth of algae until it covers the surface of the water [3], [4], which is referred to as eutrophication. Eutrophication is a neutral process in which the ecosystem has many nutrients, such as nitrogen and phosphates from agricultural areas, waste products from factory areas, and many animal carcasses, resulting in excessive algae growth. When large amounts of algae plants have covered the surface of a lake, river, or estuary, it will cause aquatic plants to die due to not getting enough sunlight for the process of photosynthesis. The high nutritional content of surface water can affect marine environments, causing low oxygen levels [5]. This condition causes the biochemical oxygen demand (BOD) to increase because the bacteria are unable to decompose organic matter due to low oxygen levels to carry out the process. High BOD levels signify degraded water quality, while low BOD levels suggest good water quality [6]. The minimal presence of oxygen causes aquatic life, such as fish, not to get enough oxygen and die.

Many studies have shown that precipitation reactions among metal ions like Mg^{2+}, Fe^{3+}, and Ca^{2+} can be used to remove phosphate chemically [7]. Phosphate can also be eliminated through the enhanced biological phosphorus removal process by polyphosphate accumulation in organisms under anaerobic/aerobic cycling [8]. However, these processes are complicated, and their cost makes both methods unattractive treatment options for wastewater treatments. Other alternatives to remove phosphate include adsorption and ion exchange. Adsorption has gained considerable attention because of its simplicity, environmental safety, and effectiveness [9]. Phosphate adsorption has been studied using low-cost sorbents like calcined Mytella falcata shells [10], calcined eggshells [11], finely ground mussel shells [12], calcined mussel shells [12], corn cob biochar [13], oyster shells [14], modified electrolytic manganese residue [15], and carbon nanotubes functionalised with L-tyrosine [16]. According to previous studies, the effectiveness rate of phosphate removal will increase as the temperature of calcine increases [17]. The efficiency will grow higher until it becomes constant at a specific time when the adsorption has reached equilibrium.

Even if a variety of low-cost adsorbents have been implemented to remove phosphate from water, the use of calcined marsh clam shells (CMCs) in removing phosphate in water with verification using kinetic and isotherm models needs to be scrutinised. The objectives of this study are (1) to investigate the removal efficiency of phosphate from an aqueous solution using waste marsh clam shells calcined at different temperatures and (2) to analyse the adsorption process using kinetic and isotherm models based on the batch experiment data.

2. Materials and Methods

2.1 Preparation of Adsorbent

Waste marsh clam shells were obtained from Kelantan, Malaysia. The shells were thoroughly washed with tap water to cleanse of impurities [18]. The shells were dried in the sun for 2 days and then baked for 2 days at 30°C [19]. The adsorbents were then ground and sieved for 1.18–2.36 mm particle size. The shells were calcined for 2 hours using a furnace at 4 variety of temperatures: 500, 600, 700, and 800°C [20].

2.2 Preparation of Aqueous Solution

Potassium dihydrogen phosphate (KH_2PO_4) was used to make the aqueous phosphate solution. An aqueous solution containing 100 ppm of phosphate was set up by adding 0.1433 g of (KH_2PO_4) in 1 L of deionised water and diluted until a solution concentration of 10 mg/L was obtained.

2.3 Batch Experiment

A total of 10 conical flasks were used in the batch experiment, each containing 100 mL of KH_2PO_4 solution with 2 g of adsorbents added. The flasks were stirred on an orbital shaker at 170 rpm. Ten samples were taken at 5, 10, 15, 20, 25, 30, 40, 50, 65, and 95 min. The samples were filtered through a filter pump to remove suspended solids [21].

2.4 Analytical Method

A UV–vis spectrophotometer (HACH DR6000) was implemented to identify the concentration of phosphate from the samples. A scanning electron microscope (SEM; COXEM EM-30AX PLUS) was implemented to determine the porosity and surface shape of the adsorbent, while energy dispersive X-ray fluorescence (EDXRF) was utilised to identify the chemical and percentage composition in the CMCs. Fourier transform infrared spectroscopy (FTIR;

Int. Journal of Integrated Engineering Vol. 16 No. 9 (2024) p. 67-79

Spectrum Two FTIR Spectrometer, Perkin Elmer) was employed to determine the CMCs before and after phosphorus adsorption. The crystalline structure composition of the adsorbent was assessed by implementing X-ray diffraction (XRD; Second Generation BRUKER D2 Phaser Benchtop).

3. Results and Discussion

The influences of contact duration and calcination temperature of CMCs on the removal efficiency of phosphate from aqueous solution were evaluated. In addition, instrumental techniques such as FTIR, XRD, SEM, and EDXRF were used to investigate the properties of the CMC adsorbent. The data from the batch experiment were further analysed to see if they were better matched to the pseudo-first-order or pseudo-second-order kinetic models and Freundlich or Langmuir isotherm models.

3.1 Characterisation of Physical and Chemical Properties

A combination of several instrumental techniques was employed to characterise the physical and chemical features of the adsorbent before and after the process. SEM with EDXRF was used to determine the changes in the surface morphology and material porosity after calcination. FTIR was implemented before and after adsorption to assess the functional groups exist and shifts in peak position and intensity. XRD was employed to investigate the structural changes and the development of new crystallographic structures produced by phosphate adsorption.

3.1.1 SEM and EDXRF analysis

As demonstrated by Fig. 1 for surface morphology for CMCs, the surface of adsorbents was found to have an irregular structure. Furthermore, the packing pores are mostly found in the micropore and macropore, and the surfaces of the CMCs are rough. This also shows that the adsorbent can produce well-developed pore structures after calcination. Because the adsorbate must first pass through those pores before reaching the adsorptive site, pores of various sizes and shapes may affect adsorption efficiency [22]. According to batch experiments, the analysis proved the potential of phosphorus removal using CMCs with the existence of element composition, as shown in Table 1.

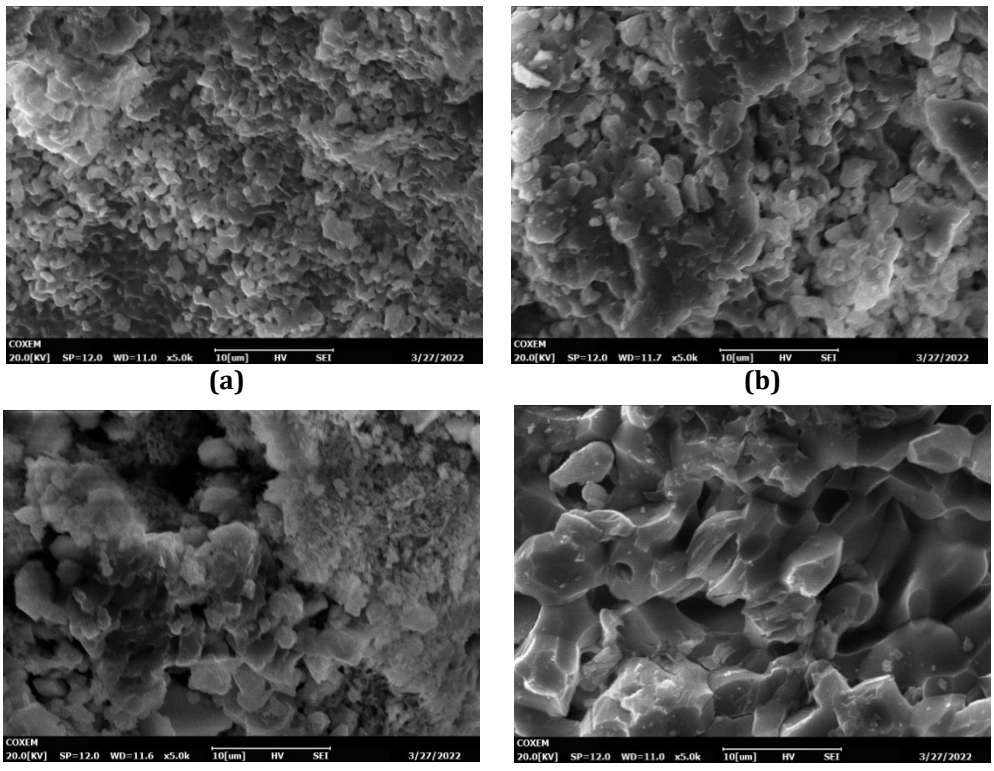

Fig. 1 *SEM micrographs at 5000× magnification for CMCs calcined at (a) 500; (b) 600; (c) 700; and (d) 800 ℃*

The most predominant elements in CMCs, shown in Table 1, were calcium and oxygen. Calcium content increased proportionally with increasing calcination temperature, with a minimum weight of 24.20% (500°C) and

a maximum weight of 57.65% (800°C). Meanwhile, the oxygen concentration decreased correspondingly. Calcium-containing substances are capable to eliminate phosphates from an aqueous solution [23]. Ultimately, all shell samples in the experiment have the ability to adsorb phosphates due to the presence of a calcium-positive charge for every calcine adsorbent to attract a phosphate-negative charge in a water solution.

Table 1 *Elemental composition of CMCs*

Temperature (°C)	500	600	700	800
Elements	Weight %			
Ca	24.20	31.16	36.83	57.65
O	52.70	49.87	47.56	35.21
Na	3.02	2.59	NA	NA
Au	3.71	15.58	3.04	2.77

3.1.2 FTIR Analysis

FTIR spectrometer was implemented to determine the functional groups [24] of CMCs, as shown in Fig. 2. Table 2 displays the FTIR spectra of CMCs calcined at 600 °C before and after phosphate adsorption. The frequency difference for CMCs ranged from −11.81 to 0.01 cm^{-1}. The P stretching band in the FTIR spectra of CMCs is positioned and formed according to the type and spot of the surface functional groups [13].

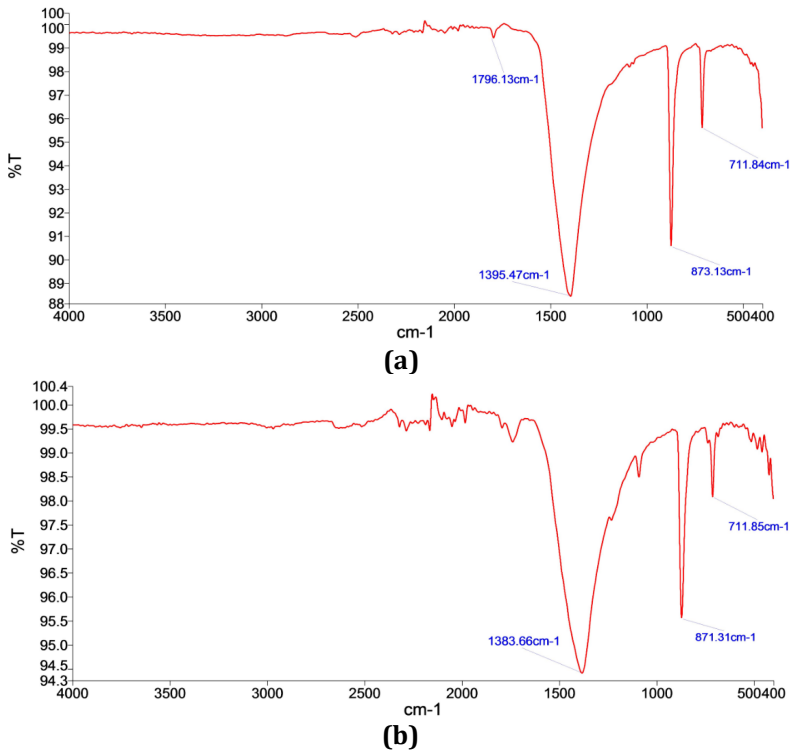

Fig. 2 *FTIR spectra of CMCs (a) Before; and (b) After adsorption*

Table 2 *FTIR spectra of CMCs before and after phosphate adsorption*

Before adsorption (cm^{-1})	After adsorption (cm^{-1})	Differences (cm^{-1})	Functional group detection	Reference
711.84	711.85	0.01	C–Cl bending	[25], [26]
873.13	871.31	−1.82	C–Cl bending	
1395.47	1383.66	−11.81	N=O bending	
1796.13	-	-	C=O stretching	

Int. Journal of Integrated Engineering Vol. 16 No. 9 (2024) p. 67-79

Before phosphate adsorption, the CMC frequencies were 711.84, 873.13, 1395.47, and 1796.13 cm^{-1}. After the adsorption, the CMC frequencies changed to 711.85, 871.31, and 1383.66 cm^{-1}, respectively. Due to the interaction between phosphate and C–Cl functional groups, the phosphate adsorption from aqueous solution onto the surface of CMCs generated a shift of 0.01 cm^{-1} (711.85–711.84 cm^{-1}), indicating alkyl halides group, and −1.82 cm^{-1} (871.31–873.13 cm^{-1}) in the C–Cl bending frequency spectrum after phosphate absorbed through CMCs. The frequency spectrum difference of −11.81 cm^{-1} (1383.66–1395.47 cm^{-1}) is linked to the N=O bending indicated nitro compounds. In contrast, the last peak is 1796.13 cm^{-1} before phosphate adsorption is attributed to C=O stretching vibrations indicated carbonyl group that was replaced by the phosphate removal.

3.1.3 XRD Analysis

XRD was employed to recognize the changes in adsorbent structure generated by novel crystallographic structures enhanced through phosphate adsorption [27], [28]. The XRD pattern exhibited in Fig. 3 shows that calcite (88%) and magnesium (12%) are the main components for CMCs calcined at 600°C. According to a previous study, the mineral composition of calcine eggshell content of calcite and hydroxylapatite was 38% and 62.0%, respectively [29]. The potential of calcite and magnesium components on the adsorbent's surface can absorb the phosphate in a water solution [30]. Also, the content of high positive charge elements such as calcium and magnesium can absorb the phosphate as a negative charge component [31].

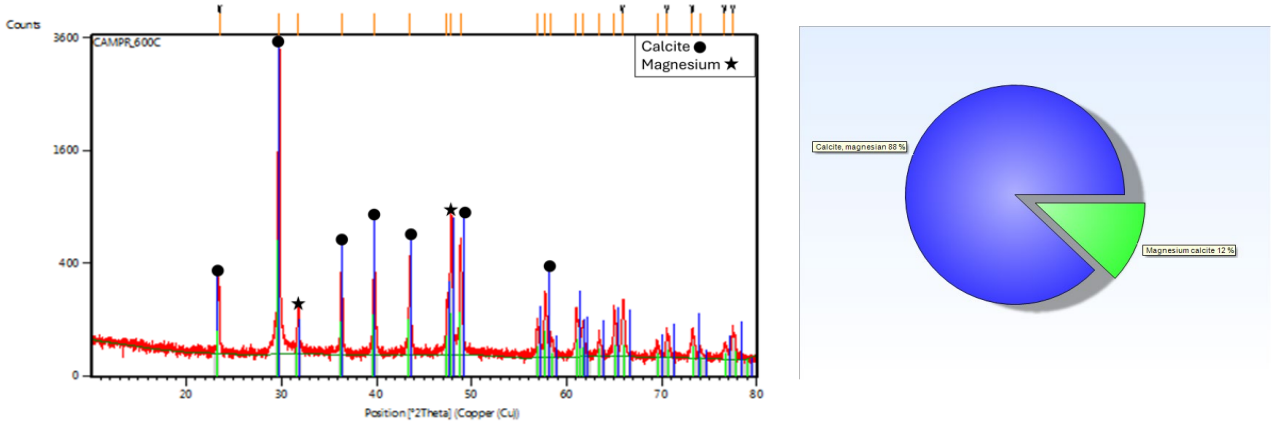

(a) **(b)**

Fig. 3 *XRD patterns for CMCs: (a) Graphic; and (b) Distribution of CMCs*

3.2 Adsorption Capacity, q (mg/g) and Removal Efficiency, E (%) of Phosphate

The calcination temperature of the CMCs contributed significantly to determine the adsorption capacity towards phosphate [32]. Batch experiments were performed to acquire the adsorption capacity of CMCs calcined at various temperatures (Fig. 4) to determine the sample that shows the highest phosphate removal [33]. The result shows a satisfactory performance for CMCs at 600°C with the highest adsorption capacity and high removal efficiency. However, still 700°C and 800°C show satisfactory performance, while the removal efficiency is more than 90%. According to SEM, the thermal activation surface breaks in Fig. 1 [34]. There is a possibility that surface cracks include atoms with weak coordination [35] at CMCs at 600°C. The EDX result shows that calcium concentration increased with temperature, while oxygen concentration decreased proportionally for all samples [36] at 600°C. However, for the sample calcined at 600°C, carbon atoms were released when the temperature was increased attributable to the rise in the kinetic energy of the atoms, causing the carbon component to decrease. The FTIR spectra of the adsorbent shown in Table 2 show significant changes before and after adsorption. The intensity of carbonate peaks was modified after phosphate adsorption, showing the depletion of carbonate and the generation of new phosphate minerals [37]. This signifies that the phosphate was introduced into the material subsequent to the adsorption. The XRD results in Fig. 3 show that calcite and lime crystals can microprecipitate in the form of $P–PO_4^{3-}$ [38]. The strength of the initial XRD peaks of the pure CMCs degraded after phosphate adsorption. The adsorption capacity can be calculated using an equation written as (1), and the removal efficiency is computed using the equation (2).

$$q = \frac{(C_i - C_f) \times V}{m} \quad (1)$$

$$E = \frac{C_i - C_f}{C_i} \times 100\% \quad (2)$$

where C_i and C_f are the initial and final concentrations of phosphate (mg/L), V is the volume of the solution (L), and m represents the mass of the adsorbent (g) [39] – [41], respectively.

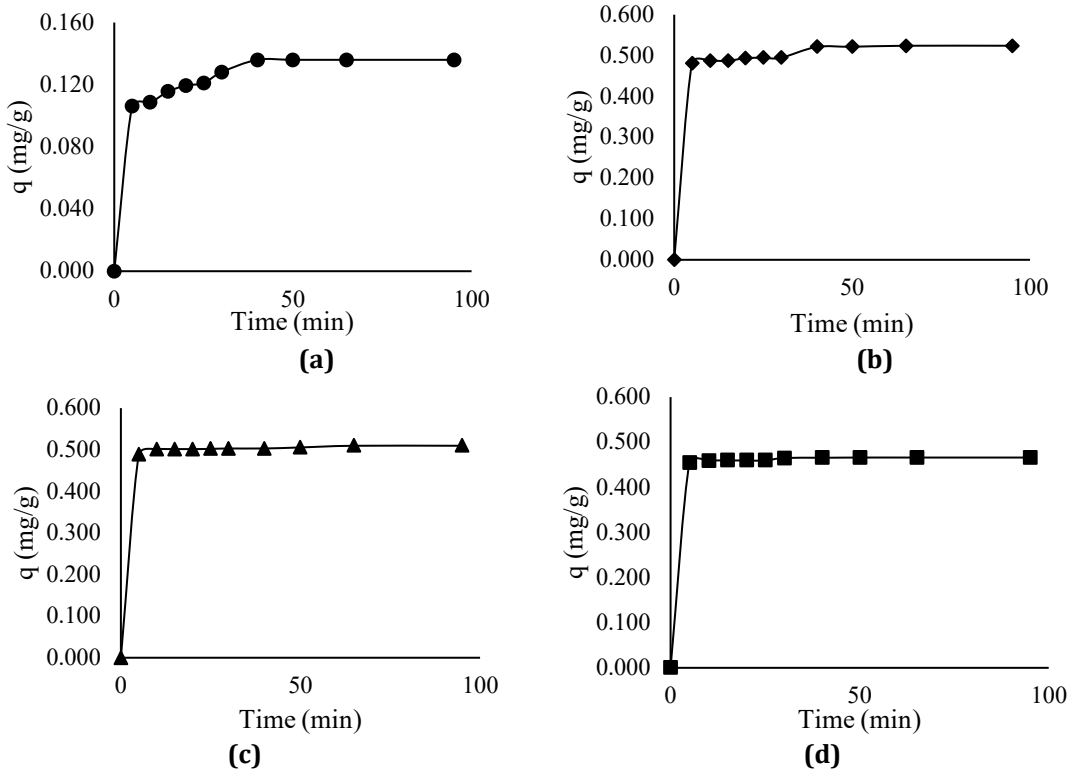

Fig. 4 *Adsorption capacity of CMCs calcined at (a) 500; (b) 600; (c) 700; and (d) 800 ℃*

Fig. 5 shows that as time increased, the removal efficiency of phosphorus increased. CMC calcined at 600°C showed the highest removal efficiency (99.53%), followed by CMCs calcined at 500°C (26.28%), 700°C (97.89%), and 800°C (92.37%). Therefore, a stable and well-determined calcination temperature can increase the removal efficiency of phosphate. After phosphate adsorption, as shown in Table 2, the strength of carbonate peaks changed, suggesting carbonate loss and the creation of new phosphate minerals. This indicates that following adsorption, phosphate was integrated into the substance. Calcite magnesium can microprecipitate $P–PO_4^{3-}$, according to our XRD results (Fig. 3). After phosphate adsorption, the intensity of the first XRD peaks of pure CMCs degraded [41]. According to SEM (Fig. 1), the thermal activation surface cracks [42]. Atoms with poor coordination may be seen in surface fissures. Calcium content rises with temperature, according to the EDX study.

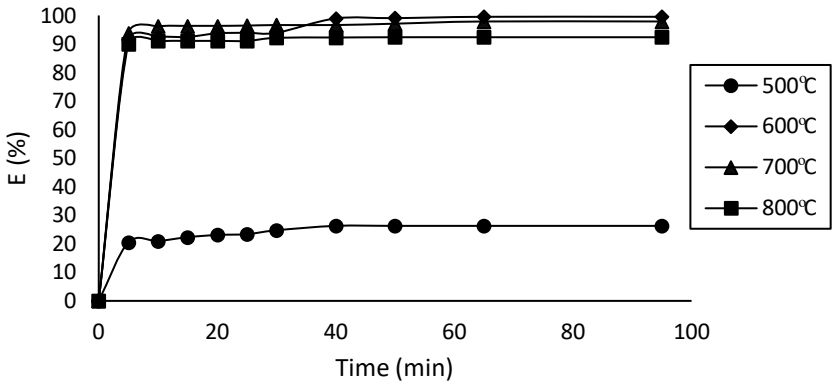

Fig. 5 *Removal efficiency, E (%) for every temperature*

Int. Journal of Integrated Engineering Vol. 16 No. 9 (2024) p. 67-79

For phosphorus absorption onto CMCs, a plot of removal efficiency and adsorption capacity against temperature produces the curve illustrated in Fig. 6. Initially, removal efficiency (E) increased significantly from 26.28% to 99.53%. As the calcination temperature was increased, E gradually decreased until it reached 91.4%.

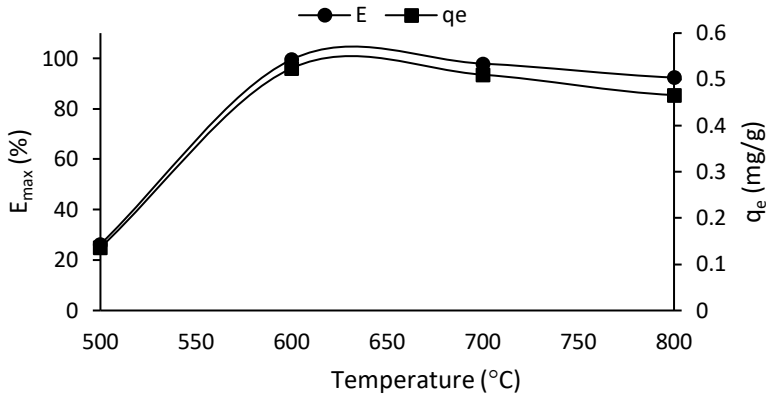

Fig. 6 *Removal efficiency, E (%) and adsorption capacity, q_e (mg/g) of CMCs calcined at different temperatures*

3.3 Adsorption Kinetic Model

Adsorption kinetic models reveal the rate and mechanism of reaction in the phosphate adsorption process and the transition from a liquid to a solid phase [43]. Two models are implemented to investigate the adsorption process for ion adsorption from a solution: pseudo-first-order (PFO) and pseudo-second-order (PSO) kinetic models [44]. Reaching adsorption equilibrium in a timely manner is an important design criteria for a cost-effective wastewater treatment system [45]. Hence, equations (3) and (4) were applied as the linear equation represented by the graph to plot the graph for the PFO and PSO models, respectively.

$$\ln[q_e - q_t] = \ln q_e - k_1 t \tag{3}$$

$$\frac{t}{q_t} = \frac{t}{q_e} + \frac{1}{k_2 {q_e}^2} \tag{4}$$

where q_e stands for the amount of phosphate adsorbed once equilibrium is established (mg/g), q_t is the amount of phosphate adsorbed over the adsorption period (mg/g), k_1 and k_2 are rate constants of the PFO and PSO equations, respectively (min^{-1}), and t_i is the time of adsorption (min) [46]. Following that, to get the parameter error function value, F_e can be calculated using equation (5).

$$F_e = \sqrt{\left(\frac{1}{n-p}\right)\sum_{i}^{n}(q_{t(exp)} - q_{t(theo)})^2} \tag{5}$$

where n is the measurements number, p denotes the kinetic parameters number, $q_{t(exp)}$ denotes the experimental q value, and $q_{t(theo)}$ denotes the theoretical q value (mg/g). The most appropriate model should have the least F_e value and the greatest R^2 value [47]. The experimental outcomes were determined by implementing the PFO and PSO models [48]. The kinetic parameters of CMCs, which are adsorption capacity (q), rate constant (k), correlation coefficient (R^2) and error function (F_e), were calculated and are interpreted in Table 3. The $q_{e(theo)}$ value derived from the PFO model differed significantly from the q_e value derived from the experimental data. In contrast, the value from the PSO model was consistent with the value from research outcomes [49]. The R^2 values for the PSO model ranged from 0.9984 to 1, and the plot consists of straight lines (t/q_t against t) [50]. Meanwhile, the R^2 values for the PFO model ranged between 0.4802 and 0.8239, which were less than those of the PSO model. The values of q_e and R^2 discussed previously are displayed in Table 3 and Fig. 7. The fitting curves in Fig. 7 and all parameters of CMCs in Table 3 confirm that the PSO model is more appropriate for describing the kinetics of phosphate adsorption onto CMCs. This indicates that the overall rate of phosphate adsorption process is primarily controlled by chemisorption mechanism involving the exchange of electrons, covalent bonds and ions [51], [52].

Additionally, during the early stages of the kinetics process, the phosphate ions in this study are in close proximity to the active sites. Due to electron repulsion between the adsorbed ions on a substance's surface and the solution ions, equilibrium is reached after this period [53]. It is supported by instrumental techniques that have been done in which the presence of calcite and lime crystals may result in PO_4^{3-} microprecipitation. Carbonate peaks decreased in intensity and disappeared after phosphate adsorption. This suggests that new phosphate minerals were generated on the adsorbent surface. Then, the existence of atoms with poor coordination conditions may come from the surface cracks.

Table 3 *The kinetic parameters for pseudo-first-order and pseudo-second-order models*

Temperatures (°C)	$q_{e(exp)}$ (mg/g)	PFO parameters				PSO parameters			
		$q_{e(theo)}$ (mg/g)	k_1 (min^{-1})	R^2	F_e	$q_{e(theo)}$ (mg/g)	k_2 (min^{-1})	R^2	F_e
500	0.136	0.0724	0.0744	0.8239	0.8182	0.1394	3.3285	0.9984	17.7075
600	0.524	0.1744	0.0887	0.8144	4.1371	0.5287	1.9661	0.9996	12.8629
700	0.510	0.0487	0.0611	0.4802	5.3834	0.5107	6.7284	1	15.5367
800	0.466	0.0830	0.1427	0.6785	4.5778	0.4669	12.0001	1	18.8008

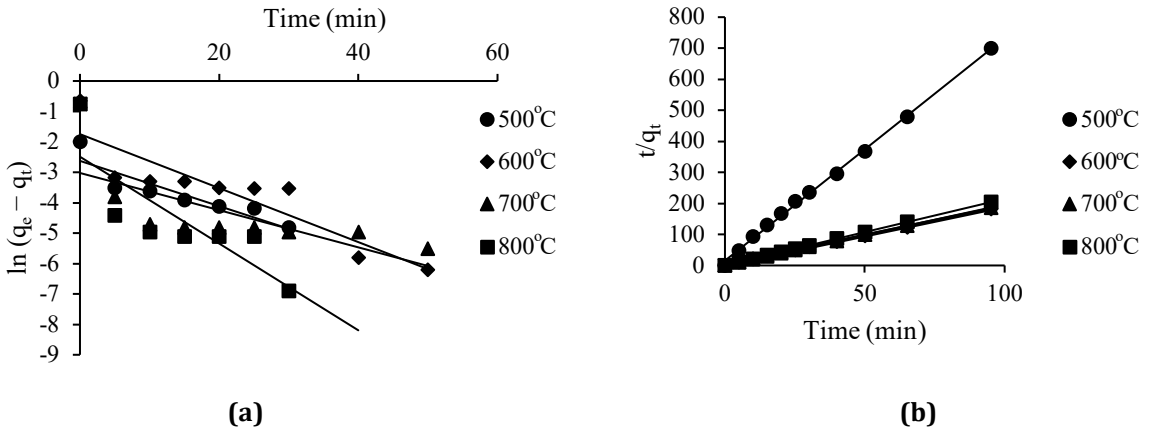

(a) **(b)**

Fig. 7 *(a) Pseudo-first-order and (b) Pseudo-second-order graph (linear regression study for the adsorption of PO_4^{3-} onto CMCs)*

3.4 Adsorption Isotherm Model

Freundlich adsorption isotherm describes the amount of gas adsorbed per unit mass [49] of solid adsorbent fluctuates with changes in system pressure at a stable temperature [54].

$$\log q_e = \log K_f + \frac{1}{n}\log C_e \tag{6}$$

where q_e is a solute sorption equilibrium concentration per gram of adsorbent (mg/g), C_e is a solute's equilibrium aqueous concentration (mg/L), and K_f is a Freundlich constant proportional to the adsorption capacity and adsorption intensity [55]. Equation (6) was used to obtain Fig. 8.

Int. Journal of Integrated Engineering Vol. 16 No. 9 (2024) p. 67-79

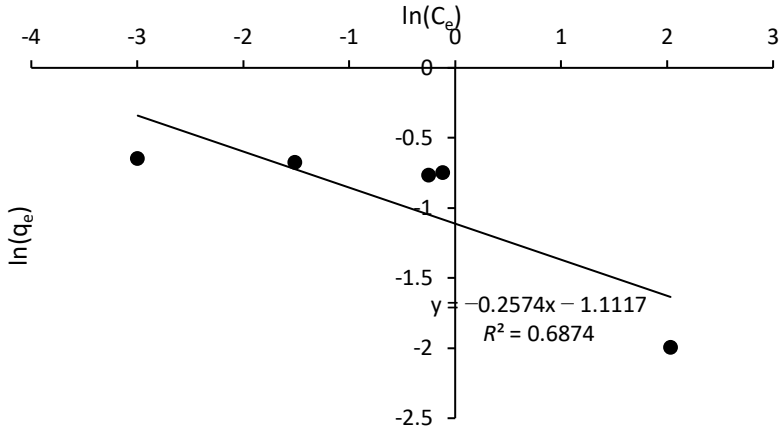

Fig. 8 *Linear line of plotting ln(q_e) versus ln(C_e) for the adsorption of PO_4^{3-} onto CMCs*

Langmuir isotherm model is utilised to model adsorption equilibrium data or determine which model is most suited for the data. The linearisation approach is the most often used method for estimating the Langmuir parameters [56].

$$\frac{C_e}{q_e} = \frac{C_e}{q_m} + \frac{1}{K_l q_m} \tag{7}$$

where K_L (L·mg^{-1}·h^{-1}) is the proportion of the adsorption and desorption rates, and q_m (mg/g) is the higher adsorption capacity anticipated by Langmuir [57]. Equation (7) was used to obtain Fig. 9.

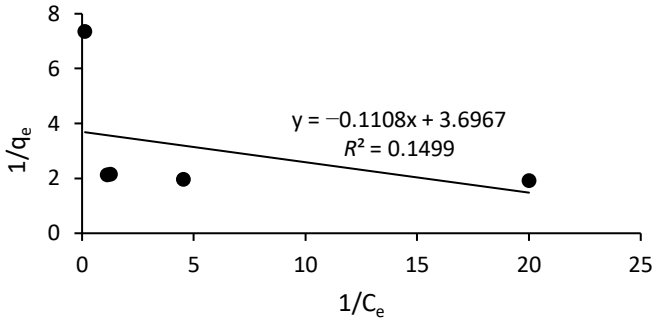

Fig. 9 *Linear line of plotting $1/q_e$ versus $1/C_e$ for the adsorption of PO_4^{3-} onto CMC*

Table 4 *Parameters for Freundlich and Langmuir isotherm models*

Freundlich Model			Langmuir Model		
n	K_F	R^2	q_{max}	K_L	R^2
−3.885	0.3290	0.6874	0.2705	−33.3651	0.1499

The Langmuir model is based on the assumption of monolayer adsorption occurring on a homogeneous surface, while the Freundlich model predicts that adsorption occurs on a heterogeneous surface. The nonlinear fitted curves and derived parameters of the isotherm models are depicted in Fig. 8 and Fig. 9, respectively. Based on Table 4, the Freundlich model provided a better fit (R^2 = 0.6874) than the Langmuir model because the Freundlich model's value of R^2 is closer to one. The R^2 coefficient is important to identify the research data corresponded perfectly with the model. The Freundlich isotherm model indicated the phosphate adsorption onto the CMCs well, which indicates multilayer adsorption of phosphate on the CMCs surface layer. Adsorption is a surface phenomenon characterised by the transfer of adsorbates to adsorbents. Humans have widely used adsorption technology for water and wastewater treatment due to its efficiency, ease of use, environmental friendliness, and low cost [58].

4. Conclusion

The research outcomes show that CMCs have the potential to be employed as an adsorbent for removing phosphate from an aqueous solution. The effect of different calcination temperatures of CMCs on the removal performance of phosphate was investigated. In addition, the data from batch experiments were analysed using kinetic and isotherms models. The highest removal efficiency was obtained using CMCs calcined at 600°C, which was 99.53%. The CMCs calcined at 600°C showed surface cracks that could cause atoms with highly defective coordination environments to be present. In addition, Ca was the major element present in that sample after O. The PSO model provided the best fit for the adsorption kinetic data, which indicates that the adsorbent contains multiple active sites. The PSO model had the greatest correlation coefficient (R^2 = 1) and the least F_e value, 12.8629, indicating that the adsorption process is chemisorption with a driving force through electron transfer between the adsorbent and the solution. The isotherm model data were accurately represented by the Freundlich model (R^2 = 0.6874), showing that phosphate adsorption onto CMCs from an aqueous solution occurs on a heterogeneous surface with multilayer sorption. To gain approval for potential practical implementations, it will also be necessary to comprehend the transfer of trace pollutants from untreated wastewater to rivers (when these materials are implemented as adsorbents). The application of different CMCs can enhance phosphate removal due to the capability of adsorption on surface materials and advanced understanding for the future development of wastewater treatment plants.

Acknowledgement

This research was supported by Universiti Tun Hussein Onn Malaysia (UTHM) through a Multidisciplinary Research Grant (MDR) Vot Q744 and GPPS (Vot Q673).

Conflict of Interest

The authors declare that there is no conflict of interest regarding the publication of the paper.

Author Contribution

The authors confirm their contribution to the paper as follows: ***study conception and design:*** *Nur Husna Muslim, Noorul Hudai Abdullah, Nur Atikah Abdul Salim, Norzainariah Abu Hassan;* ***data collection, analysis, interpretation of results, and draft manuscript preparation:*** *Abdul Aziz Maryani, Nur Aqilah Hisham, Muhammad Ariff Aiman Mohd Radzi. All authors reviewed the results and approved the final version of the manuscript.*

References

[1] Mezenner, N. Y. & Bensmaili, A. (2009) Kinetics and thermodynamic study of phosphate adsorption on iron hydroxide-eggshell waste, *Chemical Engineering Journal, 147(2-3),* 87-96, https://doi.org/10.1016/j.cej.2008.06.024

[2] Saar, K., Nõges, P., Søndergaard, M., Jensen, M., Jørgensen, C., Reitzel, K. & Jensen, H. S. (2022) The impact of climate change and eutrophication on phosphorus forms in sediment: Results from a long-term lake mesocosm experiment, *Science of The Total Environment, 825,* 153751, https://doi.org/10.1016/j.scitotenv.2022.153751

[3] Yang, J., van Lier, J. B., Li, J., Guo, J. & Fang, F. (2022) Integrated anaerobic and algal bioreactors: A promising conceptual alternative approach for conventional sewage treatment, *Bioresource Technology, 343*, 126115, https://doi.org/10.1016/j.biortech.2021.126115

[4] Yang, X., Bi, Y., Ma, X., Dong, W., Wang, X. & Wang, S. (2022) Transcriptomic analysis dissects the regulatory strategy of toxic cyanobacterium Microcystis aeruginosa under differential nitrogen forms, *Journal of Hazardous Materials, 428,* 128276, https://doi.org/10.1016/j.jhazmat.2022.128276

[5] Chen, L., Zhao, J., Zhang, Z., Shen, Z., Dong, W., Ma, R., & Zhou, A. (2022) Lake eutrophication in northeast China induced by the recession of the East Asian summer monsoon, *Quaternary Science Reviews, 281,* 107448, https://doi.org/10.1016/j.quascirev.2022.107448

[6] Quang, H. H. P., Dinh, N. T., Thi, T. N. T., Bao, L. T. N., Yuvakkumar, R. & Nguyen, V. H. (2022) Fe2+, Fe3+, Co2+ as highly efficient cocatalysts in the homogeneous electro-Fenton process for enhanced treatment of real pharmaceutical wastewater, *Journal of Water Process Engineering, 46,* 102635, https://doi.org/10.1016/j.jwpe.2022.102635

[7] Sun, S., Han, J., Hu, M., Gao, M., Qiu, Q., Zhang, S. & Ma, J. (2021) Removal of phosphorus from wastewater by Diutina rugosa BL3: Efficiency and pathway, *Science of The Total Environment, 801,* 149751, https://doi.org/10.1016/j.scitotenv.2021.149751

[8] Wang, R., Yang, C., Hu, H., Yang, Q. & Du, B. (2021) The impact of the varying nutrient concentrations on the enhanced biological phosphorus removal performance and functional phosphorus-accumulating and denitrifying genes in an anaerobic-aerobic–anoxic sequencing batch reactor, *Environmental Technology & Innovation, 21,* 101256, https://doi.org/10.1016/j.eti.2020.101256
[9] Makita, Y., Sonoda, A., Sugiura, Y., Ogata, A., Suh, C., Lee, J. H. & Ooi, K. (2020) Phosphorus removal from model wastewater using lanthanum hydroxide microcapsules with poly (vinyl chloride) shells, *Separation and Purification Technology, 241,* 116707, https://doi.org/10.1016/j.seppur.2020.116707
[10] Henrique, D. C., Quintela, D. U., Ide, A. H., Erto, A., da Silva Duarte, J. L. & Meili, L. (2020) Calcined Mytella falcata shells as alternative adsorbent for efficient removal of rifampicin antibiotic from aqueous solutions, *Journal of environmental chemical engineering, 8(3),* 103782, https://doi.org/10.1016/j.jece.2020.103782
[11] Santos, A. F., Arim, A. L., Lopes, D. V., Gando-Ferreira, L. M. & Quina, M. J. (2019) Recovery of phosphate from aqueous solutions using calcined eggshell as an eco-friendly adsorbent, *Journal of environmental management, 238*, 451-459, https://doi.org/10.1016/j.jenvman.2019.03.015
[12] Paradelo, R., Conde-Cid, M., Cutillas-Barreiro, L., Arias-Estévez, M., Nóvoa-Muñoz, J. C., Álvarez-Rodríguez, E. & Núñez-Delgado, A. (2016) Phosphorus removal from wastewater using mussel shell: Investigation on retention mechanisms, *Ecological Engineering, 97,* 558-566, https://doi.org/10.1016/j.ecoleng.2016.10.066
[13] Binh, Q. A. & Nguyen, H. H. (2020) Investigation the isotherm and kinetics of adsorption mechanism of herbicide 2, 4-dichlorophenoxyacetic acid (2, 4-D) on corn cob biochar, *Bioresource Technology Reports, 11,* 100520, https://doi.org/10.1016/j.biteb.2020.100520
[14] Martins, M. C., Santos, E. B. & Marques, C. R. (2017) First study on oyster-shell-based phosphorous removal in saltwater—A proxy to effluent bioremediation of marine aquaculture, *Science of the Total Environment, 574*, 605-615, https://doi.org/10.1016/j.scitotenv.2016.09.103
[15] Shu, J., Liu, R., Wu, H., Liu, Z., Sun, X. & Tao, C. (2018) Adsorption of methylene blue on modified electrolytic manganese residue: kinetics, isotherm, thermodynamics and mechanism analysis, *Journal of the Taiwan Institute of Chemical Engineers, 82,* 351-359, https://doi.org/10.1016/j.jtice.2017.11.020
[16] Saxena, M., Sharma, N. & Saxena, R. (2020) Highly efficient and rapid removal of a toxic dye: adsorption kinetics, isotherm, and mechanism studies on functionalised multiwalled carbon nanotubes, *Surfaces and Interfaces, 21,* 100639., https://doi.org/10.1016/j.surfin.2020.100639
[17] Yan, Y., Sun, X., Ma, F., Li, J., Shen, J., Han, W. & Wang, L. (2014) Removal of phosphate from etching wastewater by calcined alkaline residue: Batch and column studies, *Journal of the Taiwan Institute of Chemical Engineers, 45,* 4, 1709-1716, https://doi.org/10.1016/j.jtice.2013.12.023
[18] Bastami, K. D., Hamzepoor, A., Raeisi, H., Bagheri, H., Baniamam, M., & Rahnama, R. (2021) Biogenic silica, eutrophication risk and different forms of phosphorus in surface sediments of Anzali wetland, Caspian Sea, *Marine Pollution Bulletin, 173*, 113138, https://doi.org/10.1016/j.marpolbul.2021.113138.
[19] Salim, N. A. A., Puteh, M. H., Yusoff, A. R. M., Abdullah, N. H., Fulazzaky, M. A., Rudie Arman, M. A. Z. & Zainuddin, N. A. (2020) Adsorption isotherms and kinetics of phosphate on waste mussel shell, *Malaysian Journal of Fundamental and Applied Sciences, 16, 3,* 393-399, https://doi.org/10.11113/mjfas.v16n3.1752
[20] Yan, S., Huo, W., Yang, J., Zhang, X., Wang, Q., Wang, L. & Huang, Y. (2018) Green synthesis and influence of calcined temperature on the formation of novel porous diatomite microspheres for efficient adsorption of dyes, *Powder Technology, 329,* 260-269, https://doi.org/10.1016/j.powtec.2018.01.090
[21] Huang, X. L., Zhao, F., Qi, Y., Qiu, Y. A., Chen, J. S., Liu, H. K. & Wang, Z. M. (2021) Red phosphorus: A rising star of anode materials for advanced K-ion batteries, *Energy Storage Materials, 42,* 193-208, https://doi.org/10.1016/j.ensm.2021.07.030.
[22] Zuo, X., Wang, L., He, J., Li, Z., & Yu, S. (2014) SEM-EDX studies of SiO2/PVDF membranes fouling in electrodialysis of polymer-flooding produced wastewater: Diatomite, APAM and crude oil, *Desalination, 347,* 43-51, https://doi.org/10.1016/j.desal.2014.05.020.
[23] Nguyen, T. A. H., Ngo, H. H., Guo, W. S., Nguyen, T. T., Vu, N. D., Soda, S. & Cao, T. H. (2020) White hard clam (Meretrix lyrata) shells as novel filter media to augment the phosphorus removal from wastewater, *Science of the Total Environment, 741,* 140483, https://doi.org/10.1016/j.scitotenv.2020.140483.
[24] Migliavacca, D. M., Teixeira, E. C., Gervasoni, F., Conceição, R. V. & Rodriguez, M. T. R. (2009) Characterisation of wet precipitation by X-ray diffraction (XRD) and scanning electron microscopy (SEM) in the metropolitan area of Porto Alegre, Brazil, *Journal of Hazardous Materials, 171(1-3),* 230-240, https://doi.org/10.1016/j.jhazmat.2009.05.135.
[25] Nandiyanto, A. B. D., Oktiani, R. & Ragadhita, R. (2019) How to read and interpret FTIR spectroscope of organic material, *Indonesian Journal of Science and Technology, 4(1), 97*-118, https://doi.org/10.17509/ijost.v4i1.15806
[26] Abdullah, N. H., Adnan, N. A., Mohd Rashidi, N. F. N., Yaacob, M. S. S. & Abdul Salim, N. A. (2022) Comparing the adsorption isotherms and kinetics of phosphate adsorption on various waste shells as adsorbent, *Water Practice & Technology, 17(5),* 974-985, https://doi.org/10.2166/wpt.2022.051

[27] Howard, K. T., Benedix, G. K., Bland, P. A. & Cressey, G. (2011) Modal mineralogy of CM chondrites by X-ray diffraction (PSD-XRD): Part 2. Degree, nature and settings of aqueous alteration, *Geochimica et Cosmochimica Acta, 75(10),* 2735-2751, https://doi.org/10.1016/j.gca.2011.02.021
[28] Liu, T., Chen, X., Wang, X., Zheng, S. & Yang, L. (2018) Highly effective wastewater phosphorus removal by phosphorus accumulating organism combined with magnetic sorbent MFC@ La (OH) 3, *Chemical Engineering Journal, 335,* 443-449., https://doi.org/10.1016/j.cej.2017.10.117
[29] Lee, J. I., Kim, J. M., Yoo, S. C., Jho, E. H., Lee, C. G. & Park, S. J. (2022) Restoring phosphorus from water to soil: Using calcined eggshells for P adsorption and subsequent application of the adsorbent as a P fertiliser, *Chemosphere, 287,* 132267, https://doi.org/10.1016/j.chemosphere.2021.132267
[30] Ren, C., Li, Y. F., Zhou, Q. & Li, W. (2021) Phosphate uptake by calcite: Constraints of concentration and pH on the formation of calcium phosphate precipitates, *Chemical Geology, 579,* 120365, https://doi.org/10.1016/j.chemgeo.2021.120365
[31] Fan, B., Ding, J., Fenton, O., Daly, K., Chen, S., Zhang, S. & Chen, Q. (2022) Investigation of differential levels of phosphorus fixation in dolomite and calcium carbonate amended red soil, *Journal of the Science of Food and Agriculture*, *102, 2,* 740-749, https://doi.org/10.1002/jsfa.11405
[32] Lee, J. I., Kim, J. M., Yoo, S. C., Jho, E. H., Lee, C. G. & Park, S. J. (2022) Restoring phosphorus from water to soil: Using calcined eggshells for P adsorption and subsequent application of the adsorbent as a P fertiliser, *Chemosphere, 287,* 132267, https://doi.org/10.1016/j.chemosphere.2021.132267.
[33] Paradelo, R., Conde-Cid, M., Cutillas-Barreiro, L., Arias-Estévez, M., Nóvoa-Muñoz, J. C., Álvarez-Rodríguez, E. & Núñez-Delgado, A. (2016) Phosphorus removal from wastewater using mussel shell: Investigation on retention mechanisms, *Ecological Engineering, 97,* 558-566, https://doi.org/10.1016/j.ecoleng.2016.10.066
[34] Shen, Y., Zhuang, L., Zhang, J., Fan, J., Yang, T. & Sun, S. (2019) A study of ferric-carbon micro-electrolysis process to enhance nitrogen and phosphorus removal efficiency in subsurface flow constructed wetlands, *Chemical Engineering Journal, 359,* 706-712, https://doi.org/10.1016/j.cej.2018.11.152
[35] Luo, P., Liu, F., Liu, X., Wu, X., Yao, R., Chen, L. & Wu, J. (2017) Phosphorus removal from lagoon-pretreated swine wastewater by pilot-scale surface flow constructed wetlands planted with Myriophyllum aquaticum. *Science of the Total Environment, 576,* 490-497, 2017, https://doi.org/10.1016/j.scitotenv.2016.10.094
[36] Jiang, J., Kim, D. I., Dorji, P., Phuntsho, S., Hong, S. & Shon, H. K. (2019) Phosphorus removal mechanisms from domestic wastewater by membrane capacitive deionisation and system optimisation for enhanced phosphate removal, *Process Safety and Environmental Protection, 126,* 44-52, https://doi.org/10.1016/j.psep.2019.04.005
[37] Nguyen, T. A. H., Ngo, H. H., Guo, W. S., Nguyen, T. H. H., Soda, S., Vu, N. D. & Pham, T. T. (2020) White hard clam (Meretrix lyrata) shells media to improve phosphorus removal in lab-scale horizontal sub-surface flow constructed wetlands: Performance, removal pathways, and lifespan, *Bioresource Technology, 312,* 123602, https://doi.org/10.1016/j.biortech.2020.123602
[38] Nguyen, T. A. H., Ngo, H. H., Guo, W. S., Nguyen, T. T., Vu, N. D., Soda, S. & Cao, T. H. (2020) White hard clam (Meretrix lyrata) shells as novel filter media to augment the phosphorus removal from wastewater, *Science of the Total Environment, 741,* 140483, https://doi.org/10.1016/j.scitotenv.2020.140483
[39] Tarayre, C., De Clercq, L., Charlier, R., Michels, E., Meers, E., Camargo-Valero, M. & Delvigne, F. (2016) New perspectives for the design of sustainable bioprocesses for phosphorus recovery from waste, *Bioresource Technology, 206,* 264-274, https://doi.org/10.1016/j.biortech.2016.01.091
[40] Walton, C. R., Shorttle, O., Jenner, F. E., Williams, H. M., Golden, J., Morrison, S. M. & Pasek, M. (2021) Phosphorus mineral evolution and prebiotic chemistry: From minerals to microbes, *Earth-Science Reviews, 221, 103806*, https://doi.org/10.1016/j.earscirev.2021.103806
[41] Wang, R., Yang, C., Hu, H., Yang, Q. & Du, B. (2021) The impact of the varying nutrient concentrations on the enhanced biological phosphorus removal performance and functional phosphorus-accumulating and denitrifying genes in an anaerobic-aerobic–anoxic sequencing batch reactor, *Environmental Technology & Innovation, 21,* 101256, https://doi.org/10.1016/j.eti.2020.101256
[42] Singh, S., Anil, A. G., Khasnabis, S., Kumar, V., Nath, B., Adiga, V. & Ramamurthy, P. C. (2022) Sustainable removal of Cr (VI) using graphene oxide-zinc oxide nanohybrid: Adsorption kinetics, isotherms and thermodynamics, *Environmental Research, 203,* 111891, https://doi.org/10.1016/j.envres.2021.111891
[43] Babapour, M., Dehghani, M. H., Alimohammadi, M., Arjmand, M. M., Salari, M., Rasuli, L. & Khan, N. A. (2022) Adsorption of Cr (VI) from aqueous solution using mesoporous metal-organic framework-5 functionalised with the amino acids: Characterisation, optimisation, linear and nonlinear kinetic models, *Journal of Molecular Liquids, 345,* 117835, https://doi.org/10.1016/j.molliq.2021.117835
[44] Yan, Y., Sun, X., Ma, F., Li, J., Shen, J., Han, W. & Wang, L. (2014) Removal of phosphate from etching wastewater by calcined alkaline residue: Batch and column studies, *Journal of the Taiwan Institute of Chemical Engineers, 45(4), 1709*-1716, https://doi.org/10.1016/j.jtice.2013.12.023

[45] Wu, F. C., Tseng, R. L., Huang, S. C. & Juang, R. S. (2009) Characteristics of pseudo-second-order kinetic model for liquid-phase adsorption: A mini-review, *Chemical Engineering Journal, 151(1-3),* 1-9, https://doi.org/10.1016/j.cej.2009.02.024
[46] Salim, N. A. A., Fulazzaky, M. A., Zaini, M. A. A., Puteh, M. H., Khamidun, M. H., Yusoff, A. R. M. & Nuid, M. (2021) Phosphate removal from wastewater in batch system using waste mussel shell, *Biointerface Res. Appl. Chem., 11(4), 11473*-11486, https://doi.org/10.33263/BRIAC114.1147311486
[47] Binh, Q. A. & Nguyen, H. H. (2020) Investigation the isotherm and kinetics of adsorption mechanism of herbicide 2, 4-dichlorophenoxyacetic acid (2, 4-D) on corn cob biochar, *Bioresource Technology Reports, 11,* 100520, https://doi.org/10.1016/j.biteb.2020.100520
[48] Simonin, J. P. (2016) On the comparison of pseudo-first order and pseudo-second order rate laws in the modeling of adsorption kinetics, *Chemical Engineering Journal, 300,* 254-263, https://doi.org/10.1016/j.cej.2016.04.079
[49] Salim, N. A. A., Puteh, M. H., Yusoff, A. R. M., Abdullah, N. H., Fulazzaky, M. A., Rudie Arman, M. A. Z. & Zainuddin, N. A. (2020) Adsorption isotherms and kinetics of phosphate on waste mussel shell. Malaysian *Journal of Fundamental and Applied Sciences, 16(3),* 393-399, https://doi.org/10.11113/mjfas.v16n3.1752
[50] You, K., Yang, W., Song, P., Fan, L., Xu, S., Li, B. & Feng, L. (2022) Lanthanum-modified magnetic oyster shell and its use for enhancing phosphate removal from water, *Colloids and Surfaces A: Physicochemical and Engineering Aspects, 633,* 127897, https://doi.org/10.1016/j.colsurfa.2021.127897
[51] Kabir, M. M., Akter, M. M., Khandaker, S., Gilroyed, B. H., Didar-ul-Alam, M., Hakim, M. & Awual, M. R. (2022) Highly effective agro-waste based functional green adsorbents for toxic chromium (VI) ion removal from wastewater, *Journal of Molecular Liquids, 347,* 118327, https://doi.org/10.1016/j.molliq.2021.118327
[52] Salim, N. A. A., Abdullah, N. H., Khairuddin, M. R., Arman, M. A. B. Z. R., Khamidun, M. H., Fulazzaky, M. A. & Puteh, M. H. (2018) Adsorption of phosphate from aqueous solutions using waste mussel shell, *In MATEC Web of Conferences, 250,* 06013
[53] Ncibi, M. C. (2008) Applicability of some statistical tools to predict optimum adsorption isotherm after linear and nonlinear regression analysis, *Journal of Hazardous Materials, 153(1-2),* 207-212, https://doi.org/10.1016/j.jhazmat.2007.08.038
[54] Li, X., Wang, K. & Peng, Y. (2018) Exploring the interaction of silver nanoparticles with pepsin and its adsorption isotherms and kinetics, *Chemico-biological interactions, 286,* 52-59, https://doi.org/10.1016/j.cbi.2018.03.004
[55] Abdullah, N. H., Liom, S. L., Zainudin, A. H., Huzil, M. A. I., Yaacob, M. S. S., Salim, N. A. A. & Talaiekhozani, A. (2022) Waste Mussel Shells as an Adsorbent for Phosphate Removal in Solution: Kinetic and Isotherm Model, *International Journal of Nanoelectronics & Materials, 15*, 25-36.
[56] Al-Ghouti, M. A. & Da'ana, D. A. (2020) Guidelines for the use and interpretation of adsorption isotherm models: A review, *Journal of hazardous materials, 393,* 122383, https://doi.org/10.1016/j.jhazmat.2020.122383
[57] Sharmin, A., Hai, M. A., Hossain, M. M., Rahman, M. M., Billah, M. B., Islam, S. & Smith, G. C. (2020) Reducing excess phosphorus in agricultural runoff with low-cost, locally available materials to prevent toxic eutrophication in hoar areas of Bangladesh, *Groundwater for sustainable development, 10,* 100348, https://doi.org/10.1016/j.gsd.2020.100348
[58] Salari, H., Erami, M., Dokoohaki, M. H. & Zolghadr, A. R. (2022) New insights into adsorption equilibrium of organic pollutant on MnO2 nanorods: Experimental and computational studies, *Journal of Molecular Liquids, 345,* 117016, https://doi.org/10.1016/j.molliq.2021.117016